Intra- and Interband Free-Carrier Absorption and the Fundamental Absorption Edge in n-Type InP

W. P. Dumke, M. R. Lorenz, and G. D. Pettit

IBM Watson Research Center, Yorktown Heights, New York 10598

(Received 7 January 1970)

The infrared absorption in n-type InP was studied as a function of free-carrier concentration from 3.5×10^{17} to $\sim10^{19}$ cm^{-3} in the spectral range of 10 μ to the fundamental absorption edge. The Burstein shifted edge, the normal intraband free-carrier absorption, and the interband free-carrier absorption were analyzed. The fundamental edge shifts to higher energy with increasing free-carrier concentration but only by 47% of the expected Burstein shift. The energy separation between the central-conduction-band minimum and the next higher conduction valleys in InP was found to be 0.90 ± 0.02 eV.

INTRODUCTION

Recently, Lorenz *et al.*[1] reported on the band structure and the direct transition electroluminescence in the $In_{1-x}Ga_xP$ alloys. Part of this study consisted of measuring the intervalley conduction-band transitions in InP in order to understand the energy-gap variation in the alloy system. The free-carrier absorption (FCA) provides a direct measure of the energy difference of the high-mobility conduction-band minimum (Γ_{1c}) and the next higher conduction-band minima. Similar studies have been reported on GaAs by Balslev[2] and by Spitzer and Whelan[3] and in the $In_{1-x}Ga_xSb$ alloy system by Lorenz *et al.*[4] In addition, interconduction-band transitions have been treated theoretically by Haga and Kimura.[5]

Higher-lying conduction-band minima are of theoretical interest in band-structure calculations, for they provide a check on the accuracy of the first-principles calculations. They have even greater importance in the determination of the energy-gap variation in ternary alloy systems, as has been demonstrated in the $In_{1-x}Ga_xP$ system for visible light emission[1] or in the $In_{1-x}Ga_xSb$ system for predicting and observing the Gunn effect.[4] An accurate determination of the energy difference between different sets of conduction-band minima is quite difficult. Aside from utilizing optical free-carrier absorption to find the energy difference, electrical transport properties as a function of hydrostratic pressure can be analyzed in terms of a multiband conduction model. The present work was undertaken to study in greater detail the dependence of the optical absorption in n-type InP from 10 μ to the fundamental absorption edge. This is in part a reinvestigation of the earlier work but over a wider range of donor concentrations and involving a more complete evaluation of the materials studied.

The optical absorption of interest to us can be divided into three separate processes. They are shown in Fig. 1. The normal free-carrier absorption α_{FC} depends on wavelengths approximately as

$$\alpha_{FC} \propto \lambda^n \quad . \tag{1}$$

For photon energies, $\hbar\omega \gtrsim \Delta E$, the interconduction band absorption, α_{IB}, begins. Here ΔE is the energy difference between the conduction-band minimum at $\vec{k}=(0, 0, 0)$ and the next higher set of conduction-band minima. The final process of interest is the valence-band–to–conduction-band absorption α_{VC}. In all three absorption processes, the occupation of the conduction-band states must be taken into account. In the following section these processes will be examined in some detail.

EXPERIMENTAL

InP was prepared from its high-purity constit-

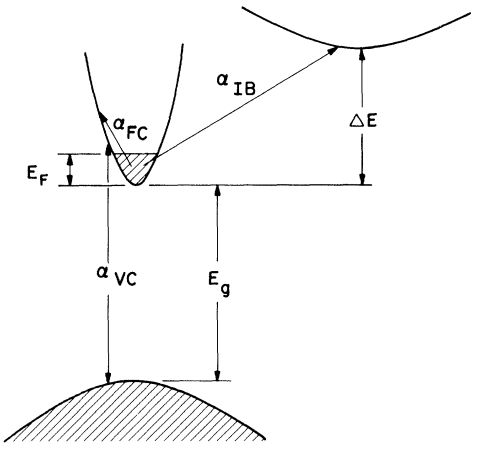

FIG. 1. Schematic energy-band diagram showing the absorption coefficients due to intraband free-carrier absorption α_{FC}, interband free-carrier absorption α_{IB}, and fundamental edge absorption α_{VC}. E_g is the energy gap, E_F is the Fermi level, and ΔE is the energy separation between the central minimum and the next higher-lying conduction-band valleys.

uent elements by a modified two-zone Bridgman drop technique.[6] Solid and sound, but polycrystalline, ingots 1.5 cm o.d. and approximately 7 cm long were obtained. Typical grain sizes ranged from 1 to 5 mm. The ingots were doped with various amounts of Te. The donor impurity concentration along the growth axis increased from the first-to-grow tip to the last-to-grow tail, indicating that Te in the InP has a segregation coefficient less than unity, similar to its behavior in other III-V compounds.[7]

The ingots were cut into a series of three wafer sets. The central wafer of each set was used for the optical measurement while the two flanking wafers were used for electrical characterization.

Resistivity and Hall coefficients at 77 and 300 °K were measured on Van der Pauw samples using conventional techniques. The carrier concentrations were calculated by assuming that $n = (R_H ec)^{-1}$.

Optical measurements consisted of measuring the transmission of mechanically polished wafers at 77 °K in the range from 10 to about 0.8 μ. The initial polished wafer thicknesses were about 0.5 cm. By successive lapping and polishing, we were able to get reproducible overlapping curves of absorption coefficients up to 4×10^3 cm^{-1}. Since there was always a small donor concentration gradient across the thickness of the wafer, we lapped off equivalent amounts from each surface in the process of reducing the wafer thickness.

The absorption coefficient was calculated from the optical transmission according to

$$T = (1-R)^2 e^{-\alpha x}/(1-R^2 e^{-2\alpha x}) \ , \qquad (2)$$

where T is the transmission, α is the absorption coefficient in cm^{-1}, and x is the thickness of the sample. We used a constant value of $R = 0.28$ for the reflectivity.

RESULTS

The carrier concentrations of the various specimens used for optical measurements are given in Table I. The numbers are based on the electron concentration of slices adjacent to the optical specimen. Each value given is the average of the two measurements with the error showing the maximum deviation across the optical slice.

TABLE I. Absorption coefficient α at 4 μ for samples of various electron concentration n, and the corresponding optical capture cross sections per electron $\sigma = \alpha/n$.

Sample identification	Electron concentration (10^{18} cm^{-3})	α(4 μ) (cm^{-1})	σ(4 μ) (10^{-18} cm^2)
A	0.35 ± 0.01	1.55	4.4
B	0.71 ± 0.04	4.1	5.8
C	1.65 ± 0.05	9.0	5.5
D	2.1 ± 0.4	14.3	6.8
E	5.7 ± 0.2	36	6.3
F	9.6 ± 0.5	75	7.8

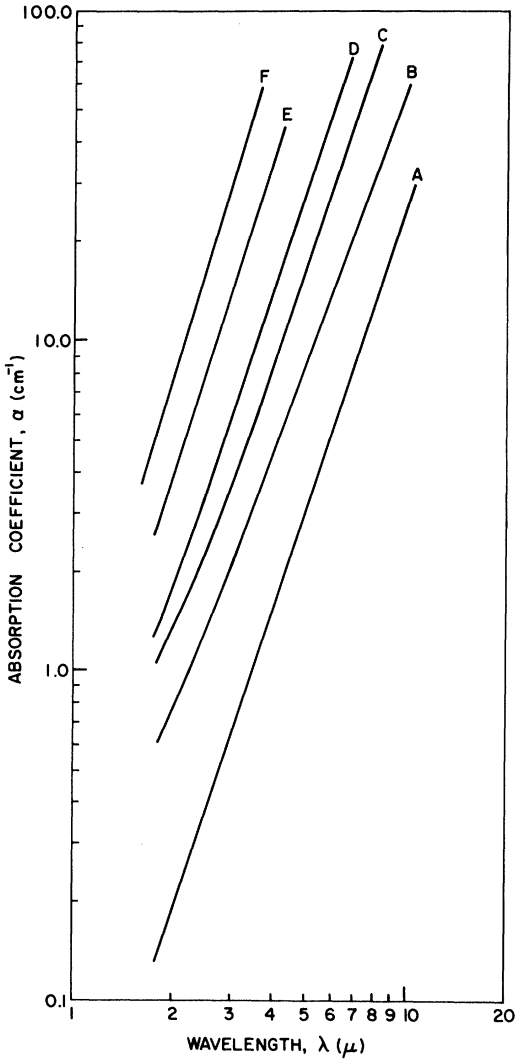

FIG. 2. Free-carrier absorption in n-type InP at 77 °K. The carrier concentration for the six different samples are given in Table I.

Absorption coefficients as a function of wavelength in the 2- to 10-μ range for the six samples studied are shown in Fig. 2. The curves are labeled corresponding to the sample identification given in Table I. The same labeling will be used throughout. All six curves are linear except for *B*, *C*, and *D* which show a slight deviation at $\lambda < 3$ μ. The value of α at $\lambda = 4$ μ is also given in Table I for each sample.

The log of α versus photon energy is given in

Figs. 3 and 4. The heavy solid lines are the measured absorption coefficients. The experimental data at the fundamental absorption edge (not shown here) extend to as high as 4×10^3 cm^{-1}. This represents the upper limit of α, above which we were unable to handle the thin samples.

ANALYSIS AND DISCUSSION

Although our primary concern is in the interband free-carrier absorption (α_{IB}), we shall also discuss the longer-wavelength intraband free-carrier absorption (α_{FC}) and the Burstein shift[8] of the fundamental absorption edge. We shall treat these three processes in reverse order.

Fundamental Absorption Edge

We have evaluated the Burstein shift approximately by considering the shift with doping of that photon energy for which the absorption is 10^3 cm^{-1}. This was the highest value of α for which we had completely reliable data for all six samples. In Fig. 5 we have plotted $\hbar\omega$ for $\alpha = 10^3$ cm^{-1} versus the impurity concentration. Absorption data by Turner and Reese[9] taken on lightly doped n-type InP (5×10^{15} cm^{-3}) show a sharp peak at 1.4095 eV, 77 °K at an α of 1.5×10^4 cm^{-1}. They interpret the peak as being due to exciton formation and calculate an exciton binding energy of 0.004 eV. This locates the energy gap at 77 °K at 1.4135 eV. The photon energy for which they observed an α of 10^3 cm^{-1} was 1.402 eV. Their value is shown in Fig. 5 and is seen to be in reasonable agreement with the data from our lowest-doped sample.

TABLE II. Fermi level, the energy separation (ΔE) of the central minimum and the next higher conduction-band valleys and the adjustable parameter C.

Sample identification	Electron concentration (10^{18} cm^{-3})	E_F (eV)	ΔE (eV)	C
A	0.35	0.027	0.90	115
B	0.71	0.044	0.90	120
C	1.65	0.074	0.91	85
D	2.1	0.087	0.91	85
E	5.7	0.16	0.91	70
F	9.6	0.22	0.92	80

We have evaluated the Fermi level of our six samples, and their values of E_F are shown in Table II. The Fermi level was calculated for a hyperbolic band with a 1.41-eV gap and a 0.065 effective-mass ratio. A reasonable fit to the experimental points in Fig. 5 is provided by a func-

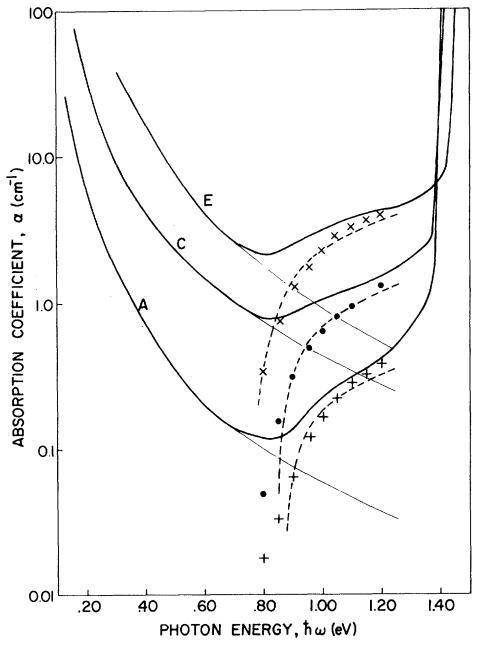

FIG. 3. Absorption coefficients as a function of photon energy $\hbar\omega$ from about 10 μ to the fundamental absorption edge. The heavy solid lines correspond to the measured absorption coefficients α_T, the light solid lines correspond to the extrapolated free-carrier absorption α_{FC}, and the points correspond to interband absorption $\alpha_{IB} = \alpha_T - \alpha_{FC}$. The dashed curves were calculated as outlined in the section of interband absorption.

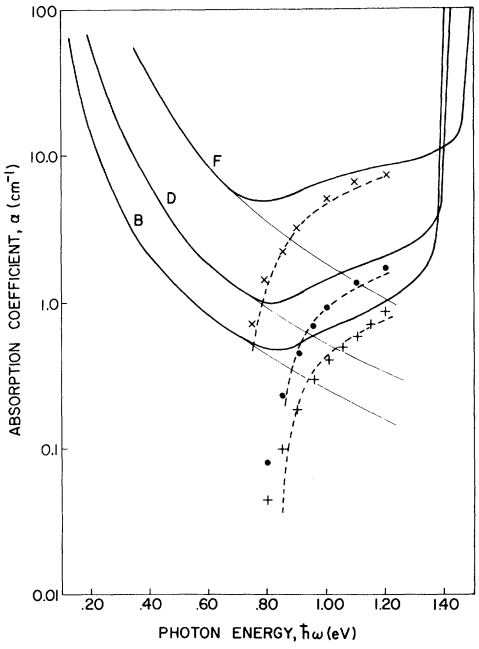

FIG. 4. Absorption coefficients as a function of photon energy $\hbar\omega$ from about 10 μ to the fundamental absorption edge. The heavy solid lines correspond to the measured absorption coefficients α_T, the light solid lines correspond to the extrapolated free-carrier absorption α_{FC}, and the points correspond to interband absorption $\alpha_{IB} = \alpha_T - \alpha_{FC}$. The dashed curves were calculated as outlined in the section of interband absorption.

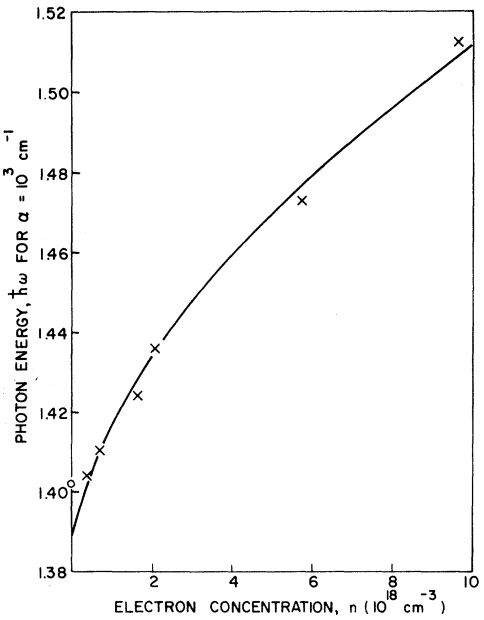

FIG. 5. Shift of the fundamental absorption edge with increasing free-carrier concentration. The crosses are the experimental values, the solid curve is given by Eq. (3) and the circled point at $n \sim 0$ is that of Ref. 9.

tion $E(n)$ which increases with the Fermi level according to

$$E(n) = 1.388 \text{ eV} + 0.55 E_F \ . \tag{3}$$

The solid curve in Fig. 5 gives the variation of $E(n)$ with carrier concentration. The shift in the absorption edge due to the Burstein effect should be of the form

$$E(n) = E_G + (1 + m_C/m_V) E_F(n) \ , \tag{4}$$

where m_C/m_V is the ratio of the conduction-band and valence-band (heavy hole) effective masses. Assuming that $m_C/m_V = 0.16$ ($m_V = 0.4 m_0$), the observed Burstein shift [Eq. (3)] is only 47% of that predicted by Eq. (4) with a constant energy gap E_G. If the density of states within the conduction band is not changing with impurity concentration, we must conclude that heavy n-type doping in InP appears to cause a decrease in the energy gap in InP of approximately 53% of the conduction-band Fermi level.

The intraband free-carrier absorption (α_{FC}) shown in Fig. 2 has a dependence very close to λ^3 over the region 3 to 10 μ. This is the same dependence observed by Balslev[2] in n-type GaAs and it is also consistent with the earlier data of Newman[10] on InP, although Newman claims his results agree with the less steep $\lambda^{5/2}$ dependence predicted by Visvanathan[11] for polar semiconductors. The absorption constant at 4 μ is given in Table I for the six samples we have investigated. The optical cross section per electron $\sigma = \alpha/n$ is also listed in Table I and its variation from sample to sample reflects partly our imperfect knowledge of the impurity concentrations and partly a contribution to the α_{FC} made by impurity scattering at the higher impurity concentrations. The mean cross section at 4 μ is 6.0×10^{-18} cm^2 and the best fit to α_{FC} for all the curves is given by $\alpha = 0.94 \times 10^{-7} n \lambda^3$ (cm^{-1}). Closer to the interband transition threshold, in the region between 0.4 and 0.8 eV, the dependence in all but the two most heavily doped samples does appear to be given by $\lambda^{5/2}$, and a $\lambda^{5/2}$ extrapolation was used to subtract out the intraband contribution to the free-carrier absorption in these samples. It should be mentioned, however, that for photon energies as large as we are considering there is no simple law which the intraband free-carrier absorption can be expected to follow.[12]

Interband Free-Carrier Absorption

The interband free-carrier absorption has been studied theoretically by Haga and Kimura.[5] An optical transition between the lowest conduction band and higher valleys not at the same point(s) in $\vec{k}$ space as the lowest band is a second-order transition which is very complicated because of the large number of virtual intermediate states the transition involves. Haga and Kimura have introduced a simplification into the theory by separating the transition into "D"-type and "I"-type processes depending on which type of intermediate state is most important. Strictly speaking, Haga and Kimura are incorrect in considering that two separate processes occur, each involving a different type of intermediate state. Actually, the contributions to the probability amplitude of the electron being in the final state involving each of the intermediate states must be added coherently and then squared in obtaining the transition probability. Nevertheless, there is considerable convenience in considering each type of "process" separately.

In the D-type process, the intermediate state is almost identical to the initial state or to the final state, and partially because of the energy denominators of $\pm\hbar\omega$ in these states the absorption incorporates a $(\hbar\omega)^{-3}$ dependence. The D-type absorption yields a narrower and more peaked band than is observed in either n-type GaAs or InP.

In the I-type process the intermediate states are in other bands below and above either the initial state or the final state depending upon whether the electromagnetic interaction is considered before or after the scattering interaction which supplies

the necessary change in wave number. The wavelength dependence of this absorption results from a density-of-states argument yielding a fairly well-defined threshold for the onset of absorption and a more slowly varying dependence of the transition probability on photon energy. The slowly varying dependence comes from two sources in the theory: (a) the $(\hbar\omega)^{-1}$ dependence from the electromagnetic interaction and (b) variations with wavelength of the energy denominators which express the extent to which energy is not conserved in a given intermediate state.

Apart from these slowly varying dependencies, the form of the absorption is given by an expression involving the densities of initial and final states. If we measure energy from the bottom of the lowest conduction minimum the density of initial filled states will be of the form

$$\frac{dn}{dE} \propto f(E) E^{1/2} h(E) , \tag{5}$$

where $h(E)$ is a ratio of the densities of states in hyperbolic and parabolic bands and is given by $h(E) = (1+E/E_G)^{1/2}(1+2E/E_G)$. The Fermi level E_F is determined by the requirement that $n = \int_0^\infty (dn/dE)dE$. ΔE is the position of the upper valleys which we will assume to have a parabolic density of states proportional to $(E-\Delta E)^{1/2}$ for $E > \Delta E$.

The absorption constant is proportional to the total transition rate for a given photon energy. If we integrate over the distributions of initial and final states, we will obtain the form of the absorption constant, apart from the more slowly varying dependence of the transition probability on photon energy, as

$$F(\hbar\omega) = \int\int E^{1/2} h(E) f(E) \times dE (E' - \Delta E)^{1/2} \delta(E' - \hbar\omega - E) dE' \tag{6}$$

or $$F(\hbar\omega) = \int dE\, f(E) E^{1/2} h(E)\, (E + \hbar\omega - \Delta E)^{1/2}.$$

This result does not take into account the relatively small gain or loss of energy due to phonon absorption and emission.

Using Eq. (6) we have fitted the observed interband FCA for the six samples with different carrier concentrations. This component of the FCA was obtained by subtracting the extrapolated intraband FCA from the data as is shown in Figs. 3 and 4. This procedure results in the largest apparent disagreement at the onset of the interband FCA, but actually the values of this absorption are very small in this region and the uncertainties in them are magnified by the use of a logarithmic vertical axis. While a reasonable fit can be obtained using $F(\hbar\omega)$ without taking into account any variation of the transition probability with energy, an improvement in the match between the theoretical and experimental curves was obtained by assuming that the absorption constant α included a factor of the form $(\hbar\omega)^{1/2}$. This corresponds to a monotonically increasing dependence of α on $\hbar\omega$ of the type which might come from the variation of energy denominators if the intermediate states of greatest importance were close to the center of the Brillouin zone and in higher conduction bands. The function we used in fitting the interband absorption data was, therefore,

$$\alpha = C(\hbar\omega)^{1/2} F(\hbar\omega), \tag{7}$$

where C is an adjustable parameter.

The Fermi levels were first calculated using a value of 0.065 for the effective-mass ratio at the bottom of the hyperbolic conduction band. This is an effective mass somewhat smaller than quoted in the literature for InP,[13,14] although it is slightly larger than what might be predicted[15] on the basis of the band gap of InP in comparison with the other direct III-V semiconductors such as GaAs. With this value, however, the values of ΔE obtained from the absorption curve fitting differ very little from sample to sample as is shown in Table II. A larger value of the effective mass than used here would have resulted in a somewhat larger spread in the values of ΔE. There is no reason to believe, however, that ΔE would be completely independent of impurity concentration since the direct band gap appears to shift significantly with doping. The variation of the magnitude of the interband FCA on the impurity concentration was in reasonable agreement with the magnitudes predicted by the expression for α. For an optimum fit, a small adjustment in the parameter C was required as is shown in Table II. These variations in the value of C are of the same relative magnitude as the variations in the intraband FCA cross section, although the correlation is not perfect between these quantities.

We have not taken into account the energy of the phonons involved in the transition. Allowing for the energy of these phonons which is likely to be at most a few hundredths of an eV, our best estimate of ΔE, the separation between the energy of the central minimum and the next higher conduction valleys in InP, is (0.90 ± 0.02) eV. There is, however, a small possibility which cannot be completely ruled out that the higher conduction valleys giving rise to the observed interband FCA are not the lowest set of higher valleys. If there were another set of valleys at an energy less than 0.90 eV above the central conduction-band minimum and if optical and scattering matrix elements

involved in transitions to these valleys were relatively small, it is possible that such states might go unnoticed in the FCA data. On the other hand, there is evidence from work on the $In_{1-x}Ga_xP$ alloys[1,16] that the lowest valleys in the Ga-rich alloys, the valleys at the point X in the Brillouin zone,[17,18] would have an energy in InP consistent with the value we have determined for ΔE. Unless some other set of valleys has moved to an even lower energy than the X point valleys as we go from GaP to InP, it seems reasonable to conclude that the valleys responsible for the interband FCA in InP are the lowest set of multiple conduction valleys.

ACKNOWLEDGMENTS

The authors wish to express their appreciation to R. Chicotka for providing the samples used in this study and to J. A. Kucza for the electrical characterization.

[1]M. R. Lorenz, W. Reuter, W. P. Dumke, R. J. Chicotka, G. D. Pettit, and J. M. Woodall, Appl. Phys. Letters 13, 421 (1968).
[2]J. Balslev, Phys. Rev. 173, 762 (1968).
[3]W. G. Spitzer and J. M. Whelan, Phys. Rev. 114, 59 (1959).
[4]M. R. Lorenz, J. C. McGroddy, T. S. Plaskett, and S. Porowski, IBM J. Res. Develop. 13, 583 (1969).
[5]E. Haga and H. Kimura, J. Phys. Soc. Japan 19, 1596 (1964).
[6]S. E. Blum, R. J. Chicotka, and B. K. Bischoff, J. Electrochem. Soc. 115, 32 (1968).
[7]*Compound Semiconductors*, edited by R. K. Willardson and H. L. Ghering (Rheinhold, New York, 1962), Vol. I.
[8]E. Burstein, Phys. Rev. 93, 632 (1954).
[9]W. J. Turner, W. E. Reese, and G. D. Pettit, Phys. Rev. 136, A1467 (1964).
[10]R. Newman, Phys. Rev. 111, 1518 (1958).
[11]S. Visvanthan, Phys. Rev. 120, 376 (1960).
[12]W. P. Dumke, Phys. Rev. 124, 1813 (1961).
[13]E. D. Palik and R. F. Wallis, Phys. Rev. 123, 131 (1961).
[14]T. S. Moss and A. K. Walton, Physica 25, 1142 (1959).
[15]F. H. Pollack, C. W. Higginbotham, and M. Cardona, J. Phys. Soc. Japan 21, 20 (1966).
[16]C. Hilsum and C. Porteous, *Proceedings of the Ninth International Conference on the Physics of Semiconductors* (Nauka Publishing House, Moscow, 1968), p. 1214.
[17]R. Zallen and W. Paul, Phys. Rev. 134, A1628 (1964).
[18]Y. L. Yarnell, J. L. Warren, R. G. Wenzel, and P. J. Dean, *Neutron Inelastic Scattering* (International Atomic Energy Agency, Vienna, 1968), Vol. 1, p. 301.

PHYSICAL REVIEW B VOLUME 1, NUMBER 12 15 JUNE 1970

Valley-Orbit Interaction in Semiconductors*

A. Baldereschi
Department of Physics, University of Illinois, Urbana, Illinois 61801
(Received 8 December 1969)

We consider the hypothesis that the valley-orbit interaction provides a sizable contribution to the observed splittings of the donor ground state in many-valley semiconductors. The effects of this interaction on the ground state of group-V donors in Si and Ge are estimated within the effective-mass theory and compared to central-cell corrections. It is shown that intervalley scattering effects are comparable in magnitude to central-cell corrections for donors in Si, whereas the latter are much more important for donors in Ge.

I. INTRODUCTION

It is well known[1] that the ground state of a donor impurity is split into two or more levels if the host semiconductor has many equivalent conduction-band minima at $\vec{k} \neq 0$. Spectroscopic investigations in Si,[2] Ge,[3] and AlSb[4] have provided accurate values of these splittings. The first successful theoretical investigation of impurity spectra in semiconductors was given by Luttinger and Kohn.[5] They developed the effective-mass theory and applied it to study the donor states in Si[6] taking into account the anisotropy of the conduction band near its six equivalent conduction-band minima. Recently Faulkner[7] has improved the variational solution of Kohn and Luttinger[6] and has shown that the effective-mass theory describes very well the excited states of the donor electron but predicts too low a binding energy for the ground state and does not explain the splittings between the ground states corresponding to different equivalent minima in the